Draft version November 30, 2023
Typeset using LaTeX twocolumn style in AASTeX631

Environmental Effects on the Galaxy Stellar Mass Function at z $\sim$ 2.5

Derek Sikorski[1]

[1] Institute for Astronomy, University of Hawaiʻi, 2680 Woodlawn Drive, Honolulu, HI 96822, USA

1. CONTEXT

Historically, galaxies have been thought to populate two distinct classes: those that are bluer, more spiral-like, and have active star formation with moderate-to-high star formation rates (SFRs); and those that are redder, more elliptical, and have little-to-no active star formation. Although efforts have been made to characterize the dominant mechanisms which may lead to the quenching of (i.e. cessation of star formation in) star forming galaxies, it is vital we understand how these mechanisms which drive star-forming galaxies to quiescence evolve with redshift. While previous studies have attempted to trace quenching in the local universe (e.g., Peng et al. 2010) and out to moderate-redshifts of z < 2 (e.g., Kawinwanichakij et al. 2017; Tomczak et al. 2017; Papovich et al. 2018; Webb et al. 2020; van der Burg et al. 2020), the development of quiescence in the high-redshift regime of $z > 2$ remains largely ambiguous.

Broadly speaking, the physical mechanisms that drive galaxy quenching can be categorized as one of two distinct processes: "mass quenching" or "environmental quenching" (Peng et al. 2010). As suggested by the name, mass quenching encapsulates processes that are directly correlated with the mass of the system. Examples may include feedback from supernovae and stellar winds (e.g., Dekel & Silk 1986), feedback from active galactic nuclei (e.g., Somerville et al. 2008), and the shock-heating of cold inflows in halos above a given mass (Dekel & Birnboim 2006). On the other hand, environmental quenching are processes which are linked to properties of the local environment in which the galaxy is situated. These processes preferentially occur in overdense environments (such as galaxy clusters), and include mechanisms such as the stripping of circumgalactic gas via ram pressure as a result of a galaxy's motion relative to the diffuse intracluster medium (e.g., Abadi et al. 1999), or an increased frequency of major galaxy-galaxy mergers (e.g., Lin et al. 2010).

One of the most important and natural ways of tracking a galaxy's evolution is via the galaxy stellar mass function (SMF). The SMF is a volume-based number density of galaxies as a function of stellar mass and will thus be affected by both mass and environmental quenching mechanisms in various ways. Using SDSS (z < 0.1) and zCOSMOS ($0.3 <$ z < 0.6), Peng et al. (2010) show that the ways in which the SMF is affected by mass and environmental quenching mechanisms are largely separable. This means there are environmental mechanisms that act to increase the quiescent fraction of galaxies, independent of the mass of the galaxies, and vice versa.

On the other hand, it has become more apparent that for $0.5 <$ z < 2.0, there is a positive correlation between the overdensity of a region and the fraction of galaxies that are quiescent in the region down to stellar-masses of $\log(M_*/M_\odot) \gtrsim 9.5$ (e.g., Kawinwanichakij et al. 2017; Tomczak et al. 2017; Papovich et al. 2018; Webb et al. 2020; van der Burg et al. 2020). Additionally, it has been shown that the environmental quenching mechanisms that drive this correlation become more efficient for higher mass galaxies (Papovich et al. 2018; van der Burg et al. 2020; Webb et al. 2020), suggesting that environmental and mass quenching do not act independently of one another. Despite this general consensus, which processes are responsible for environmental quenching remains unclear.

In this project, we will use HST observations of the Hyperion proto-supercluster at z $\sim$ 2.5 (Figure 1) to create SMFs as a function of overdensity. By comparing SMFs of quiescent galaxies in overdense regions of Hyperion with the SMF of field galaxies in underdense regions, we can constrain the importance of environmental quenching mechanisms in high-redshift, overdense regions. Additionally, by comparing the environmental dependencies of the quiescent SMF of Hyperion with the SMF of overdense regions at lower redshifts, we can constrain the timescales over which certain environmental quenching mechanisms must act. In doing so, we can develop a better understanding of the environmental quenching mechanisms that dominate at higher redshifts, the interplay of these processes with the stellar mass of the galaxies they quench, and how the efficiency of these mechanisms may evolve with redshift.

2. METHODS

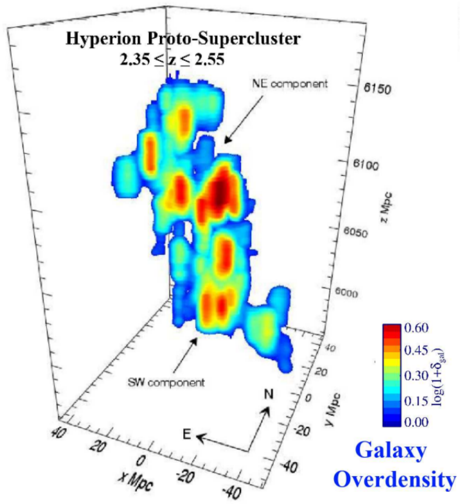

Figure 1. 3D Sky Distribution of Hyperion: A galaxy overdensity map of the Hyperion proto-supercluster (from Cucciati et al. (2018)).

In order to study the effects of environmental quenching, I will be using observations of the Hyperion proto-supercluster at z $\sim$ 2.5. The data I will be using is a combination of photometric observations from COSMOS 2020 (Weaver et al. 2022), spectroscopic data from the VIMOS Ultra Deep Survey (VUDS; Le Fèvre et al. 2015) and zCOSMOS (Lilly et al. 2007), and HST grism data. Hyperion hosts 7 distinct overdensity peaks, which are the constituent proto-groups and proto-clusters that make up the larger proto-supercluster. The ability to compare SMFs of galaxies not only with field galaxies but with galaxies within Hyperion's complex density structure makes it a unique candidate for analyzing how environments can shape the SFM of galaxy populations.

With the combined data set, I will have access to spectra of $\sim$ 250 member galaxies of Hyperion, as well as $\sim$ 300 field galaxies within the same redshift range. The galaxy sample is effectively complete in stellar mass to $\log(M_*/M_\odot) \gtrsim 9.0$ for all galaxy types (Tal et al. 2014). The first step will then be to create a color-color diagram to distinguish quiescent galaxies from star-forming galaxies, as in Figure 2. Using existing overdensity maps of Hyperion, I can then classify the fraction of quiescent galaxies as a function of overdensity to establish a general idea of how quenching efficiencies vary with environment.

The next step will be to construct the SMFs as a function of overdensity. Before doing so, I will need to fit spectral energy distributions (SEDs) to the existing spectra in order to extract the stellar masses of the galaxies. I can then create SMFs for various overdensities and quantify the interplay between environmental and mass quenching mechanisms. One way of doing this is to compare the observed SMFs to previous studies that simulated the effect of major mergers on the SMF (e.g., Tomczak et al. 2017). By comparing the observations and simulated SMFs (see Figure 3), I can constrain the integrated merging history of galaxies in various overdensity regimes.

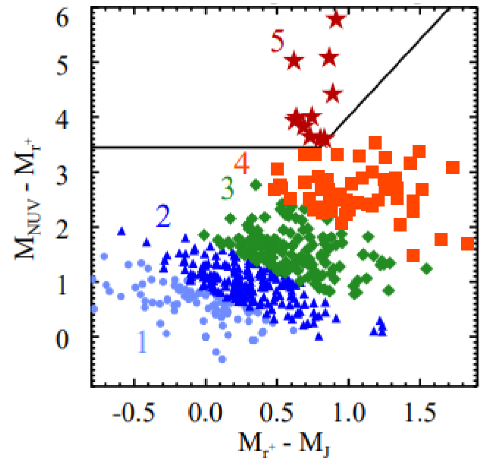

Figure 2. Predicted Quiescent Population of Hyperion: The predicted rest-frame NUVrJ color-color diagram of the Hyperion proto-supercluster, broken into 5 different color classes. The black line acts as a demarcation between galaxies that are quiescent (above) and star-forming (below). Taken from the HST proposal.

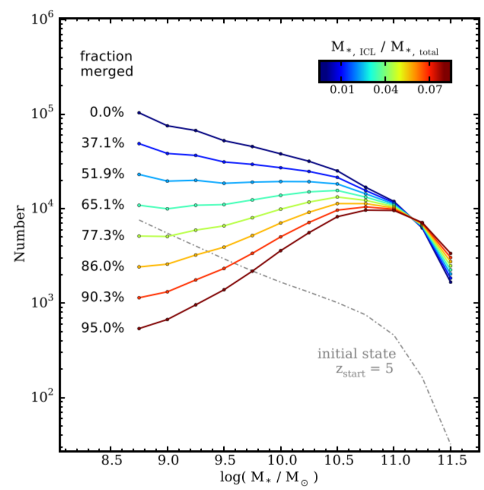

Figure 3. Effects of Mergers on the SMF: The simulated effects of mergers on SMFs, taken from Tomczak et al. (2017). The colored curves indicate different fractions of galaxies that experience mergers.

3. TIMELINE

Jan-Feb: Examine the data set, identify quiescent and star-forming populations, and begin fitting SEDs

Mar-Apr:Finish fitting SEDs and construct SMFs

May-Jun: Compare SMFs to previous observations and simulations to discern dominant quenching mechanisms and begin write-up

Jul-Aug: Finish write-up and allow time for contingencies

REFERENCES

Abadi, M. G., Moore, B., & Bower, R. G. 1999, MNRAS, 308, 947, doi: 10.1046/j.1365-8711.1999.02715.x

Cucciati, O., Lemaux, B. C., Zamorani, G., et al. 2018, A&A, 619, A49, doi: 10.1051/0004-6361/201833655

Dekel, A., & Birnboim, Y. 2006, MNRAS, 368, 2, doi: 10.1111/j.1365-2966.2006.10145.x

Dekel, A., & Silk, J. 1986, ApJ, 303, 39, doi: 10.1086/164050

Kawinwanichakij, L., Papovich, C., Quadri, R. F., et al. 2017, ApJ, 847, 134, doi: 10.3847/1538-4357/aa8b75

Le Fèvre, O., Tasca, L. A. M., Cassata, P., et al. 2015, A&A, 576, A79, doi: 10.1051/0004-6361/201423829

Lilly, S. J., Le Fèvre, O., Renzini, A., et al. 2007, ApJS, 172, 70, doi: 10.1086/516589

Lin, L., Cooper, M. C., Jian, H.-Y., et al. 2010, ApJ, 718, 1158, doi: 10.1088/0004-637X/718/2/1158

Papovich, C., Kawinwanichakij, L., Quadri, R. F., et al. 2018, ApJ, 854, 30, doi: 10.3847/1538-4357/aaa766

Peng, Y.-j., Lilly, S. J., Kovač, K., et al. 2010, ApJ, 721, 193, doi: 10.1088/0004-637X/721/1/193

Somerville, R. S., Hopkins, P. F., Cox, T. J., Robertson, B. E., & Hernquist, L. 2008, MNRAS, 391, 481, doi: 10.1111/j.1365-2966.2008.13805.x

Tal, T., Dekel, A., Oesch, P., et al. 2014, ApJ, 789, 164, doi: 10.1088/0004-637X/789/2/164

Tomczak, A. R., Lemaux, B. C., Lubin, L. M., et al. 2017, MNRAS, 472, 3512, doi: 10.1093/mnras/stx2245

van der Burg, R. F. J., Rudnick, G., Balogh, M. L., et al. 2020, A&A, 638, A112, doi: 10.1051/0004-6361/202037754

Weaver, J. R., Kauffmann, O. B., Ilbert, O., et al. 2022, ApJS, 258, 11, doi: 10.3847/1538-4365/ac3078

Webb, K., Balogh, M. L., Leja, J., et al. 2020, MNRAS, 498, 5317, doi: 10.1093/mnras/staa2752